Talanta 84 (2011) 235–239

Contents lists available at ScienceDirect

Talanta

journal homepage: www.elsevier.com/locate/talanta

Short communication

Nanomolar detection with high sensitivity microfluidic absorption cells manufactured in tinted PMMA for chemical analysis

Cedric F.A. Floquet[a,*], Vincent J. Sieben[a,b], Ambra Milani[a], Etienne P. Joly[a,3], Iain R.G. Ogilvie[a,b], Hywel Morgan[b], Matthew C. Mowlem[a]

[a] National Oceanography Centre, University of Southampton, Southampton SO14 3ZH, UK[1]
[b] Nanoscale Systems Integration Group, University of Southampton, Southampton SO17 1BJ, UK[2]

ARTICLE INFO

Article history:
Received 5 August 2010
Received in revised form
10 December 2010
Accepted 19 December 2010
Available online 25 December 2010

Keywords:
Microfluidic
PMMA
Colourimetric assays
Absorption
Microsensors

ABSTRACT

We describe a novel, cost effective and simple technique for the manufacture of high sensitivity absorption cells for microfluidic analytical systems. The cells are made from tinted polymethyl methacrylate (PMMA) in which microfluidic channels are fabricated. Two windows (typically 250 μm thick, resulting in little optical power loss) are formed at either end of the channel through which light is coupled. Unwanted stray light from the emitter passes through a greater thickness of the tinted substrate (typically the length of the cell) and is preferentially absorbed. In effect, this creates a pin-hole configuration over the length of the absorption cell, providing improved performances (sensitivity, S/N ratios, baseline noise and limit of detection) when used as an absorption cell compared to clear substrates. The method is used to achieve a LOD of 20 nM with a colourimetric iron assay and a LOD of 0.22 milli-absorption units with a pH assay.

1. Introduction

Microfluidic lab-on-a-chip (LOC) platforms [1,2] show considerable promise for the creation of robust miniaturised, high performance metrology systems with applications in diverse fields such as environmental analysis [3,4], potable and waste water, point of care diagnostics and many other physical, chemical and biological analyses. The technology allows the integration of many components and subsystems (e.g. fluidic control, mixers, lenses, light sources and detectors) in small footprint devices that could potentially be mass produced. Reduction in size enables reduction in power and reagent consumption making miniaturisation of a complete sensing system feasible. There are many applications for this technology, particularly in the development of remote *in situ* sensing systems for environmental analysis, and one area of importance is the measurement of ocean biogeochemistry [5].

Colourimetric assays for determination of inorganic chemical concentrations (e.g. nitrate/nitrite [6], phosphate [7], iron [8] and manganese [9]) have long providence and are used widely in oceanography. These colourimetric assays are used due to their suitability for measuring a wide range of analyte concentrations, including at the low levels in the open ocean [10]. Iron is of specific interest to the oceanographic community because of its key role in phytoplankton productivity and hence, carbon fixation [11–13]. Many of the traditional approaches of measuring analytes (such as iron) involve manual collection of samples with analysis in laboratory settings [14], automated and semi-automated shipboard systems [15], and *in situ* sensors [16–19] (i.e. in a submerged analytical system).

These assays operate using a common technology platform based on measuring the optical absorption of a coloured reagent, where the adsorption is proportional to the concentration of the analyte. At the heart of these techniques is the optical absorption cell.

There have been many different approaches to integration and miniaturisation of microfluidic absorption cells. Kuswandi et al. [20] and Hunt and Wilkinson [21] recently reviewed opto-fluidic integration highlighting recent advances, including absorption cell design. Many systems use optical fibres for launching and collecting light from U-shaped [22] or Z-shaped channels [23]. Whilst the fibres' numerical aperture provides a degree of stray light rejection, alignment can be problematic, especially if the goal is a low-cost mass-produced sensor. Complexity and optical power loss is also caused by coupling between fibres, sources and detectors; thereby reducing the level of integration. Grumann et al. [24] used total

* Corresponding author. Tel.: +44 023 8059 6254.
E-mail address: cfaf@noc.soton.ac.uk (C.F.A. Floquet).
[1] Tel.: +44 023 8059 6167; fax: +44 023 8059 6149.
[2] Tel.: +44 023 8059 3330; fax: +44 023 8059 3029.
[3] Now at Department of Electronic Engineering, University of Hull, Hull HU6 7RX, UK. Tel.: +44 014 8246 5384.

0039-9140/$ – see front matter © 2011 Elsevier B.V. All rights reserved.
doi:10.1016/j.talanta.2010.12.026

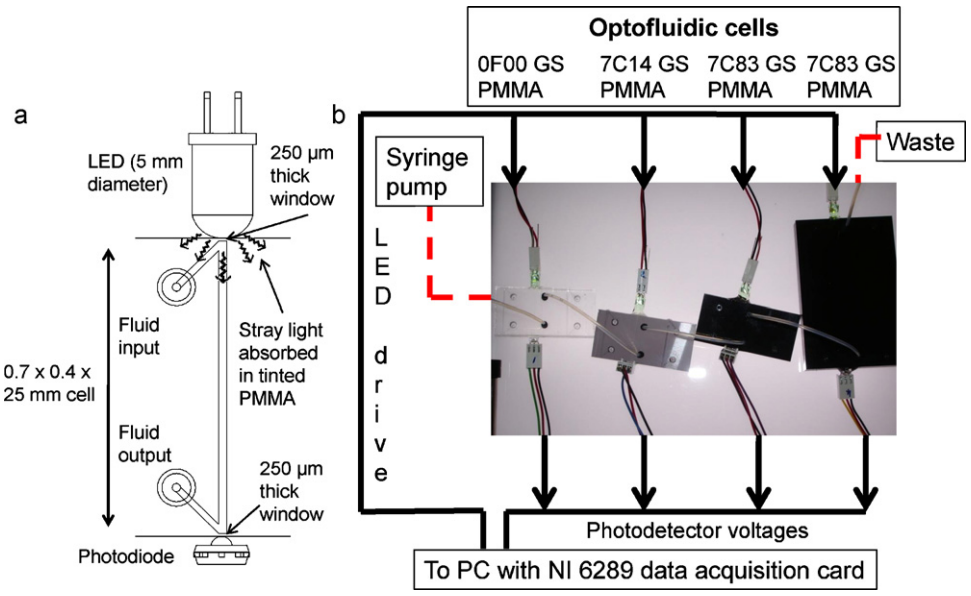

Fig. 1. (a) Schematic of an absorption cell with 250 μm thick windows. (b) Experimental setup for absorption cell evaluation. The four microfluidic cells (25 mm 0F00 GS, 25 mm 7C14 GS, 25 mm 7C83 GS and 80 mm 7C83 GS PMMA) are connected in series and a syringe pump is used to inject samples.

internal reflection at an air interface in their polymeric devices to simplify coupling of out of plane sources and detectors to 10 mm long absorption cells. Stray light reduction relied on collimation of the laser source used. Lenses have been used to increase coupling efficiencies and to reduce stray light, but require complex fabrication for relatively short (500 μm) channels [25]. The use of liquid core waveguides (LCWs) enables both long pathlengths and stray light rejection [26–29]. However, LCWs can require complex fabrication and surface treatment to maintain long-term performance [16]. Multiple reflections can be used to increase effective absorption length to greater than the geometric length [30,31], though alignment and collimation remain problematic and only short effective pathlengths are obtained. ARROW waveguide and other structures facilitating absorption detection in the evanescent wave result in short interaction lengths for a given geometric length [32]. Substrates doped with wavelength selective absorbent dyes that enable spectral filtering have been demonstrated in PDMS for optical filtering in fluorescence based systems [21,33,34]. These arrangements have not been used for colourimetric assays and the control of stray light. Novel Paired Emitter-Detector Diode detection methods [35] and low-cost lock-in detection [36] are examples of low-cost optoelectronic systems that can be used in addition to optofluidic design to further improve performance.

Despite these innovations, simple, long pathlength, robust microfluidic-based absorption cells remain elusive [37]. Jiang and Pau [38] note the challenge of creating long pathlength cells on-chip and reported a 110 mm long spiral LCW, one of the longest pathlengths on-chip. However, performance at low concentrations was impaired by refractive index changes of the analyte. Other examples of absorption cell lengths range from 50 μm to 20 mm [27,28,39–41]. These designs aimed to improve sensitivity by increasing the absorption length and reducing the amount of stray light entering the system.

We describe a novel, cost effective and simple technique for the manufacture of long pathlength absorption cells, as shown in Fig. 1. The opto-fluidic absorption cells are made using tinted substrates, which absorb stray light from both the ambient and the source. Importantly, the substrates are not completely opaque allowing coupling of light in and out of the channel through thin (250 μm) semi-transparent optical windows, manufactured at either end of the absorption cell to couple the source and detector as shown in Fig. 1a. This method simplifies manufacturing and avoids the requirement for insertion of transparent windows which would be required for totally opaque materials, and which would give dead volumes at the optofluidic junction. The optical absorption of the tinted substrate is a linear function of thickness so that there is a large ratio between absorption in the windows (typically 250 μm thick, 82% transmission) and the absorption of stray light over the length of the optical cell (25 mm, <0.01% transmission).

In effect, this creates a pin-hole configuration over the entire length of the absorption cell, which enables long pathlengths with an excellent signal to noise ratio. This results in an unprecedented limit of detection for lab-on-a-chip absorption cells.

2. Materials and methods

The devices were characterised using food dye and two colourimetric assays for both iron and pH. For the food dye and pH assay, the methods and results are described in the supplementary data. The iron assay is based on the ferrozine reagent method [8] (also see SI). Freshly prepared ferrozine was mixed with Fe^{2+} standards (0 nM, 500 nM, 1 μM, 2 μM, 4 μM, 6 μM, 10 μM) at a 1:10 mixing ratio 5 min before being injected in the opto-fluidic cells.

Opto-fluidic cells were micro-milled in different grades of PMMA (Röhm, Darmstadt, Germany): clear PMMA (0F00 GS), grey tint PMMA (7C14 GS) and dark tint PMMA (7C83 GS). Microfluidic channels, 700 μm wide and 400 μm deep, were machined leaving 250 μm thick windows. The channel cross section was a compromise between maximising the area and intensity of illumination on the active area of the photodiode, and a desire to minimise the fluidic volume; however, we have also manufactured absorption cells with cross sectional dimensions as small as 160 μm by 160 μm. Two different absorption cell designs were manufactured in this work. The first design had an absorption channel of 25 mm length, manufactured in 8 mm thick clear transparent (0F00 GS), grey (7C14 GS) or dark tinted (7C83 GS) PMMA. These three different chips were used to compare the performance of different grades of tinted-PMMA. The second design had an absorption channel length of 80 mm and was manufactured in 5 mm thick, dark tinted (7C83 GS) PMMA. The substrates, both 5 mm and 8 mm thick, showed no problems related to flexibility (Young's modulus of ~3.3 GPa); however, thinner PMMA may not be suitable for long pathlengths due

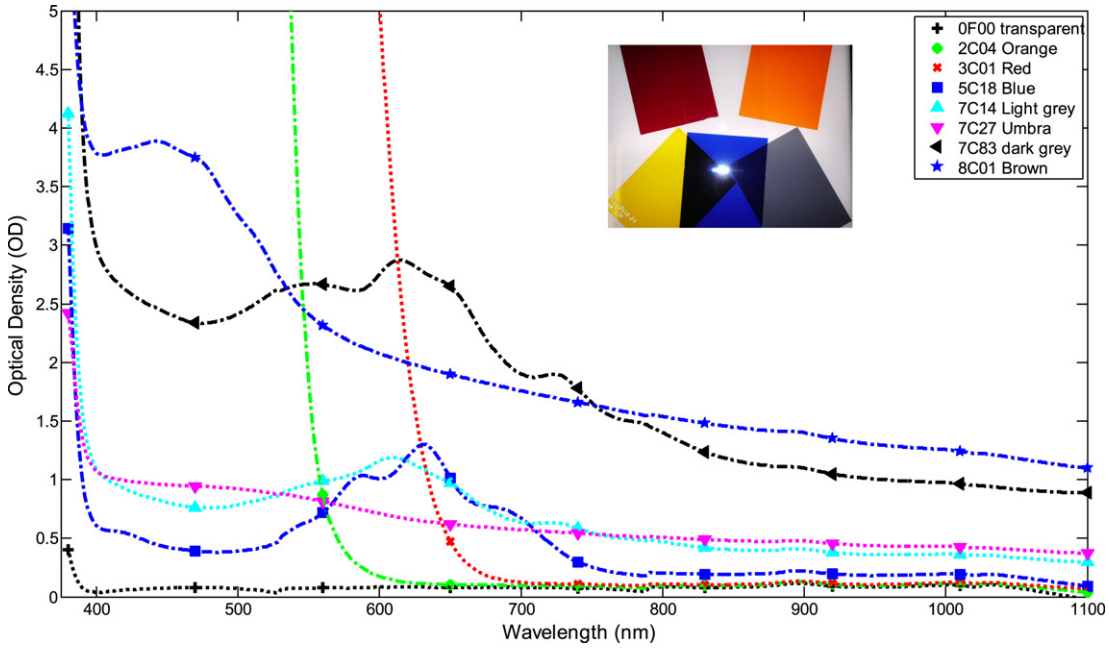

Fig. 2. Example absorbance spectra for some tinted and coloured transparent PMMA samples. The absorbance is represented in optical density. Inset: examples of commercially available coloured and tinted transparent PMMA (Rohm, Germany). Clockwise: 3C01 GS Red, 0F00 GS Transparent, 2C04 GS Orange, 7C14 GS Light grey, 5C18 GS Blue, and 1C33 GS Yellow. (For interpretation of the references to color in this figure caption, the reader is referred to the web version of the article.)

to bending of the optical path. This design demonstrates one of the longest pathlengths for microfluidic absorption spectroscopy.

A lid of identical PMMA grade was milled and solvent bonded as described previously (the process also polishes the surface of the microchannel to an optical quality) [42]. Fluidic connectors were cut in the body of the opto-fluidic cell. The optical components were aligned with a custom X Y Z stage and fixed in position with UV curable optical adhesive (Norland 68, NJ, USA). For the source, a LED centred on 562 nm (Stanley 5066X) was used. The ferrozine reagent absorption peak is centred at 562 nm with a full width half maximum (FWHM) of ~100 nm, and the LED emission peak is centred at 562 nm with a FWHM ~30 nm. A photodiode detector (TAOS TSL257, TAOS Inc., USA) was used to measure the light received at the end of the channel. We used a constant current source to drive the LED enabling a stable light output. The photodiode incorporated a built in amplifier that rejected supply noise and was powered from a precision voltage reference. These measures ensured minimal electrical noise contributions to the measured optical signals.

The complete system setup is shown in Fig. 1b. The four microfluidic chips (three 25 mm cells and one 80 mm cell) are connected in series and a syringe pump (Harvard Apparatus Nanomite, Kent, UK) is used to pump dye and samples (premixed with reagent) at a flow rate 200 μl/min. The opto-fluidic cell was rinsed with 0.1 M HCl between each standard injection. A blank measurement was also recorded to enable compensation for any drift or contamination.

Data was recorded using a National Instruments Digital Acquisition Device PCI 6289 card with a sampling rate of 110 Hz and an anti-aliasing filter set at 10 Hz. Absorption and extinction coefficient values were calculated using the common logarithmic form of the Bouguer–Beer–Lambert law. Reference spectra for the iron standards with ferrozine were obtained from a linear array photodiode spectrometer (HR4000, Ocean Optics) coupled to the same light sources used in the opto-fluidic cells. The absorption cell was a 100 mm glass cell, rinsed with MilliQ and 0.1 M HCl between each sample. Monochromatic measurements were obtained by selecting data from a single photodiode at a fixed wavelength (562 nm). Polychromatic measurements were obtained by integrating the intensity signals measured by the HR4000 over its full wavelength range.

The optical transmission of different commercially available PMMA samples was characterised, and the optical densities versus wavelength are shown in Fig. 2. PMMA absorbance spectra were obtained with a Hitachi U-28000 spectrophotometer (Hitachi, Japan) and normalised to account for the thickness of the PMMA sample. The different spectra for each grade of PMMA allows customisation of the absorption cell for the particular assay of interest.

3. Results and discussion

In this study, colourimetric assays for Fe^{2+} were performed to demonstrate the benefits of the tinted material technique over the use of clear transparent substrate. Results from the Fe^{2+} colourimetric assay are summarised in Fig. 3. Data are compared to the HR4000 spectrometer for the monochromatic and polychromatic cases.

As a measure of sensitivity, the equivalent molar absorption coefficient was calculated for all the PMMA opto-fluidic cells and compared to the theoretical value (27,900 cm^{-1} at 562 nm) [8] by calculating the slope of each curve in the linear region. This approximation gives a figure of merit representative of the performances of the system. The molar absorption coefficient for the clear transparent PMMA (0F00 GS) was 3553 cm^{-1}; for light grey (7C14 GS) it was 21,995 cm^{-1} and for the dark grey (7C83 GS) it was 22,750 cm^{-1}. Thus, the use of tinted PMMA improved the sensitivity of the system by a factor 6.4, without the need to subtract background light from the signal.

Total internal reflection (TIR) can and does occur at the substrate (refractive index (RI ~ 1.55)–air (RI ~ 1.00)) interface and also at the PMMA–water (RI ~ 1.33) interface. Therefore, in clear substrates an appreciable background signal consisting of light directly transmitted through the substrate and internally reflected light is measured by the detector. Transparent PMMA allows good light transmission, but increases the stray light that contributes to a high background measurement. This leads to a reduced measuring range, deviation from linearity (refer to supplementary data for a discussion on the

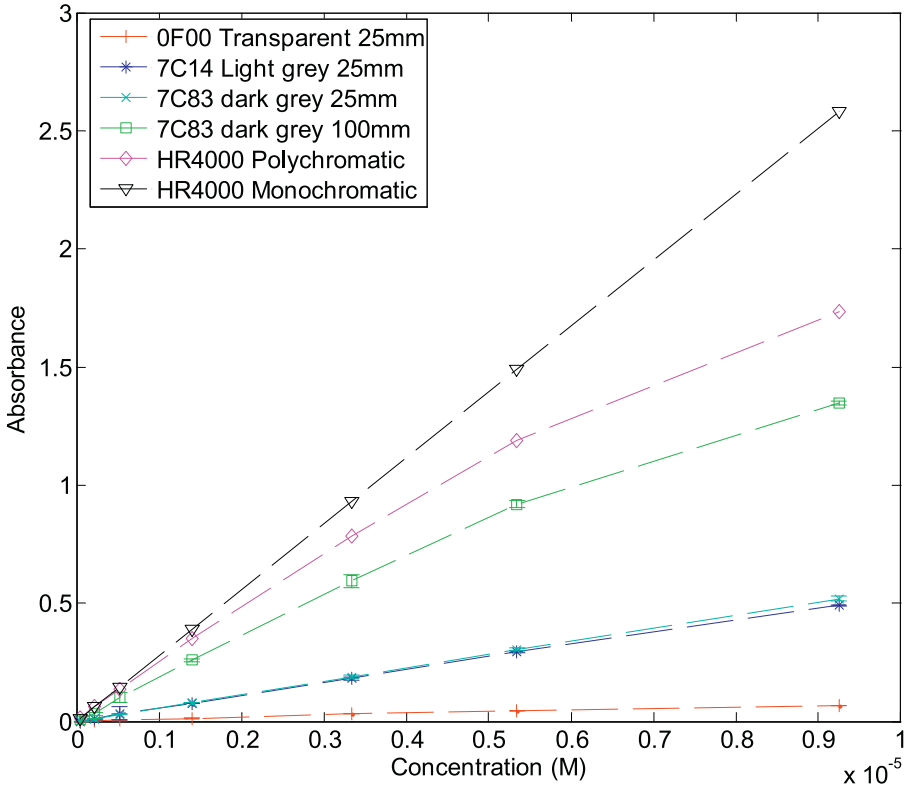

Fig. 3. Iron assay results. Comparison of the results obtained with the opto-fluidic absorption cells to measurements made using a bench-top spectrometer (Ocean Optics HR4000). Each point is the average of a triplicate measurement with its associated 95% confidence interval depicted by error bars.

impact of stray light on absorption measurements) and poor limit of detection. Even though it would be possible to subtract the background signal, this is an extra step in an automated system and can be time intensive. Other groups have used masks or pin holes to minimise the coupling of stray light into the substrate and this works to some degree [40,43]. However, the manufacturing process becomes more complex, due to difficulty in alignment and additional fabrication steps. The use of tinted or coloured transparent PMMA alleviates all these problems.

The reduction in background illumination when using the tinted-PMMA also improved the LOD; which was: clear—226 nM; light grey—33 nM, and dark grey—21 nM (all 25 mm long pathlengths). The LOD was calculated as three times the standard deviation obtained from three blank measurements [44]. For each blank measurement, MilliQ water was continuously flowed through the absorbance cell and the photodiode voltage was averaged over a 500 ms (55 points) window at the end of the injection. The use of a longer absorbance cell did not improve the LOD significantly (20 nM), due to traces of iron in the blank sample. At such low levels, an iron-free cleanroom environment would be necessary to prepare contamination free calibration standards. The small deviation from linearity observed when applying the Bouguer–Beer–Lambert law without compensation is caused by the polychromatic light source, well described in the literature [45] and shown in Fig. 3. Although the LOD did not improve with the iron assay, the sensitivity increased as expected by the ratio of pathlengths, a factor of 3.2.

To further explore the long pathlength, we investigated another colourimetric assay (pH, described in supplementary data) that was less sensitive to contamination. With the 80 mm pathlength chip, using the pH assay, we were able to achieve an LOD of 2.2×10^{-4} absorption units at 435 nm, and 9.4×10^{-4} absorption units at 592 nm, with 10 s signal averaging. For comparison, a standard UV–vis spectrophotometer (e.g. Perkin-Elmer Lambda 1050 UV-vis spectrophotometer) has a noise limit of $<0.5 \times 10^{-4}$ absorption units for 1 s integration time; however this system is based on a high sensitivity photomultiplier. Here we achieve high-performance with much less expensive optics (only LEDs and photodiodes).

4. Conclusion

We have demonstrated a novel and generic low-cost, technique for the manufacture of high performance opto-fluidic systems. The use of a coloured/tinted material to manufacture optical cells with built-in windows reduces the microfluidic chip dead volume, improves the linearity of the system (for absorbance measurements) and increases the sensitivity by a factor of 6 (minimum) when compared to clear transparent material. The technique allows for robust long pathlength absorption cells to be manufactured, obviates the need for fibre optic coupling of sources or detectors, and can potentially be extended to any tinted material or material that can be optically doped. This method of creating absorption cells is currently in use on all of our nutrient analyser systems and has implications for many research groups developing absorption based systems.

Acknowledgements

This study was supported by the UK Natural Environment Research Council (NERC) through the Oceans 2025 core programme of the National Oceanography Centre, Southampton; and by both NERC and the UK Engineering and Physical Sciences Research Council (EPSRC) through grant EP/E016774/1.

Appendix A. Supplementary data

Supplementary data associated with this article can be found, in the online version, at doi:10.1016/j.talanta.2010.12.026.

References

[1] P.S. Dittrich, K. Tachikawa, A. Manz, Analytical Chemistry 78 (2006) 3887–3907.
[2] A. Manz, N. Graber, H.M. Widmer, Sensors and Actuators B: Chemical 1 (1990) 244–248.
[3] H.-F. Li, J.-M. Lin, Analytical Bioanalytical Chemistry 393 (2009) 555–567.
[4] L. Marle, G.M. Greenway, Trace-Trends in Analytical Chemistry 24 (2005) 795–802.
[5] V.J. Sieben, C.F.A. Floquet, I.R.G. Ogilvie, M.C. Mowlem, H. Morgan, Analytical Methods 2 (2010) 484–491.
[6] P. Griess, Berichte der deutschen chemischen Gesellschaft 12 (1879) 426–428.
[7] Atkins, Journal of the Marine Biological Association of the United Kingdom 13 (1923) 119–150.
[8] L.L. Stookey, Analytical Chemistry 42 (1970), 779.
[9] C.S. Chin, K.S. Johnson, K.H. Coale, Marine Chemistry 37 (1992) 65–82.
[10] M.D. Patey, M.J.A. Rijkenberg, P.J. Statham, M.C. Stinchcombe, E.P. Achterberg, M. Mowlem, Trace-Trends in Analytical Chemistry 27 (2008) 169–182.
[11] K.H. Coale, in: J. Steele, S. Thorpe, K. Turekian (Eds.), Encyclopedia of Ocean Science, 2001.
[12] J.H. Martin, K.H. Coale, K.S. Johnson, S.E. Fitzwater, R.M. Gordon, S.J. Tanner, C.N. Hunter, V.A. Elrod, J.L. Nowicki, T.L. Coley, R.T. Barber, S. Lindley, A.J. Watson, K. Vanscoy, C.S. Law, M.I. Liddicoat, R. Ling, T. Stanton, J. Stockel, C. Collins, A. Anderson, R. Bidigare, M. Ondrusek, M. Latasa, F.J. Millero, K. Lee, W. Yao, J.Z. Zhang, G. Friederich, C. Sakamoto, F. Chavez, K. Buck, Z. Kolber, R. Greene, P. Falkowski, S.W. Chisholm, F. Hoge, R. Swift, J. Yungel, S. Turner, P. Nightingale, A. Hatton, P. Liss, N.W. Tindale, Nature 371 (1994) 123–129.
[13] J.H. Street, A. Paytan, Metal Ions in Biological Systems 43 (2005) 153–193.
[14] K.K.A.M.E.K. Grasshoff, Methods of Seawater Analysis, 3rd edition, Wiley-VCH, Weinheim, Federal Republic of Germany, 1999.
[15] F. Armstrong, C.R. Stearns, J.D. Strickland, Deep-Sea Research 14 (1967) 381.
[16] L.R. Adornato, E.A. Kaltenbacher, T.A. Villareal, R.H. Byrne, Deep-Sea Research Part I: Oceanographic Research Papers 52 (2005) 543–551.
[17] A.K. Hanson, OCEANS 2000 MTS/IEEE Conference and Exhibition, 2000, pp. 1975–1982.
[18] D. Thouron, R. Vuillemin, X. Philippon, A. Lourenco, C. Provost, A. Cruzado, V. Garcon, Analytical Chemistry 75 (2003) 2601–2609.
[19] C.M. McGraw, S.E. Stitzel, J. Cleary, C. Slater, D. Diamond, Talanta 71 (2007) 1180–1185.
[20] B. Kuswandi, J. Nuriman, W. Huskens, Verboom, Analytica Chimica Acta 601 (2007) 141–155.
[21] H.C. Hunt, J.S. Wilkinson, Microfluidics and Nanofluidics 4 (2008) 53–79.
[22] Z.H. Liang, N. Chiem, G. Ocvirk, T. Tang, K. Fluri, D.J. Harrison, Analytical Chemistry 68 (1996) 1040–1046.
[23] G.M. Greenway, S.J. Haswell, P.H. Petsul, Analytica Chimica Acta 387 (1999) 1–10.
[24] M. Grumann, J. Steigert, L. Riegger, I. Moser, B. Enderle, K. Riebeseel, G. Urban, R. Zengerle, J. Ducree, Biomedical Microdevices 8 (2006) 209–214.
[25] K.W. Ro, K. Lim, B.C. Shim, J.H. Hahn, Analytical Chemistry 77 (2005) 5160–5166.
[26] A. Datta, I.Y. Eom, A. Dhar, P. Kuban, R. Manor, I. Ahmad, S. Gangopadhyay, T. Dallas, M. Holtz, F. Temkin, P.K. Dasgupta, IEEE Sensors Journal 3 (2003) 788–795.
[27] W.B. Du, Q. Fang, Q.H. He, Z.L. Fang, Analytical Chemistry 77 (2005) 1330–1337.
[28] M.P. Duggan, T. McCreedy, J.W. Aylott, Analyst 128 (2003) 1336–1340.
[29] R. Manor, A. Datta, I. Ahmad, M. Holtz, S. Gangopadhyay, T. Dallas, IEEE Sensors Journal 3 (2003) 687–692.
[30] L. Billot, A. Plecis, Y. Chen, Microelectronic Engineering 85 (2008) 1269–1271.
[31] H. Salimi-Moosavi, Y.T. Jiang, L. Lester, G. McKinnon, D.J. Harrison, Electrophoresis 21 (2000) 1291–1299.
[32] G. Pandraud, T.M. Koster, C. Gui, M. Dijkstra, A. van den Berg, P.V. Lambeck, Sensors and Actuators A: Physical 85 (2000) 158–162.
[33] C.L. Bliss, J.N. McMullin, C.J. Backhouse, Lab on a Chip 8 (2008) 143–151.
[34] O. Hofmann, X.H. Wang, A. Cornwell, S. Beecher, A. Raja, D.D.C. Bradley, A.J. deMello, J.C. deMello, Lab on a Chip 6 (2006) 981–987.
[35] K.T. Lau, S. Baldwin, M. O'Toole, R. Shepherd, W.J. Yerazunis, S. Izuo, S. Ueyama, D. Diamond, Analytica Chimica Acta 557 (2006) 111–116.
[36] W.D. Gong, M. Mowlem, M. Kraft, H. Morgan, IEEE Sensors Journal 9 (2009) 862–869.
[37] J.Z. Pan, B. Yao, Q. Fang, Analytical Chemistry 82 (2010) 3394–3398.
[38] L.N. Jiang, S. Pau, Applied Physics Letters 90 (2007).
[39] L. Malic, A.G. Kirk, Sensors and Actuators A: Physical 135 (2007) 515–524.
[40] C. Slater, J. Cleary, K.T. Lau, D. Snakenborg, B. Corcoran, J.P. Kutter, D. Diamond, Water Science and Technology 61 (2010) 1811–1818.
[41] S. Kruanetr, S. Liawruangrath, N. Youngvises, Talanta 73 (2007) 46–53.
[42] I.R.G. Ogilvie, V.J. Sieben, C.F.A. Floquet, R. Zmijan, M.C. Mowlem, H. Morgan, Journal of Micromechanics and Microengineering 20 (2010) 065016.
[43] A. Gaspar, I. Bacsi, E.F. Garcia, M. Braun, F.A. Gomez, Analytical and Bioanalytical Chemistry 395 (2009) 473–478.
[44] L.A. Currie, Chemometrics and Intelligent Laboratory Systems 37 (1997) 151–181.
[45] C. Galli, Journal of Pharmaceutical and Biomedical Analysis 25 (2001) 803–809.